Magnetic Moments and Hyperfine-Structure Anomalies of Cs^{133}, Cs^{134}, Cs^{135}, and Cs^{137}†

H. H. STROKE,* V. JACCARINO,‡ D. S. EDMONDS, JR., AND R. WEISS
Research Laboratory of Electronics and Department of Physics, Massachusetts Institute of Technology, Cambridge, Massachusetts

(Received July 26, 1956)

The atomic-beam magnetic-resonance method was used to measure the nuclear gyromagnetic ratios and hyperfine-structure separations of the radioactive isotopes Cs^{134}, Cs^{135}, and Cs^{137}. A surface ionization detector was used.

The hyperfine-structure separations were obtained by direct $\Delta F=\pm 1$ transitions near zero field. The values of $\Delta\nu$ found for the three isotopes are:

$$\Delta\nu(Cs^{134})=10\,473.626\pm 0.015 \text{ Mc/sec},$$
$$\Delta\nu(Cs^{135})=9\,724.023\pm 0.015 \text{ Mc/sec},$$
$$\Delta\nu(Cs^{137})=10\,115.527\pm 0.015 \text{ Mc/sec}.$$

Pairs of transition belonging to the two different F-states, but involving the same m_F values, constitute frequency doublets separated by $2g_I\mu_0 H$. From measurements of the difference frequencies of these doublets for pairs of isotopes in fields in the vicinity of 9000 gauss, the following g-value ratios were obtained: $g_I(Cs^{135})/g_I(Cs^{133})=1.05820\pm 0.00008$, $g_I(Cs^{137})/g_I(Cs^{135})=1.04005\pm 0.00008$, $g_I(Cs^{134})/g_I(Cs^{133})=1.01447\pm 0.00029$.

The hfs anomalies arising from the variation of the electron wave function over the finite distribution of nuclear magnetization were calculated from these measurements. The values found for these anomalies, defined by $\epsilon_2-\epsilon_1=[g_1\Delta\nu_2(2I_1+1)]/[g_2\Delta\nu_1\times(2I_2+1)]-1$, are:

$$\epsilon(Cs^{133})-\epsilon(Cs^{135})=+0.037\pm 0.009\%,$$
$$\epsilon(Cs^{135})-\epsilon(Cs^{137})=-0.020\pm 0.009\%,$$
$$\epsilon(Cs^{133})-\epsilon(Cs^{134})=+0.169\pm 0.030\%.$$

The theory of Bohr and Weisskopf on the hfs anomalies was applied to these nuclei; the calculations are based primarily on a single-particle model with varying distributions of spin and orbital contribution to the nuclear moment. An apparent magic number effect in the anomalies was observed.

I. INTRODUCTION

THE fact that the study of the hyperfine structure of atoms in which the electron wave function has a nonzero value at the position of the nucleus would yield information about the distribution of nuclear magnetism was first recognized by Bitter[1] and by Kopfermann,[2] and treated theoretically by Bohr and Weisskopf,[3] and by Bohr.[4] The hfs splitting arising from the interaction of an $S_{\frac{1}{2}}$ atomic electron with the magnetic moment μ_I (in nuclear magnetons) of a nucleus, which is assumed to be a point-dipole, having spin I, was derived by Fermi[5] in 1933; it is given by

$$\Delta\nu=\frac{8}{3}\pi\mu_I\mu_0|\psi(0)|^2\left(\frac{2I+1}{I}\right)\frac{m}{M}, \tag{1}$$

where $\Delta\nu$ is the hyperfine-structure interaction, $\psi(0)$ is the electron wave function at the position of the nucleus, and m and M are the electron and proton masses, respectively. If one now assumes that the nucleus has a uniform charge distribution, then the electron density varies approximately as $1-(ZR^2)/a_0R_0)$ inside the nucleus. Consequently, if the nuclear magnetism is assumed to be distributed over the volume of the nucleus, then the hfs interaction would be expected to be reduced by an amount

$$\epsilon=-(ZR_0/a_0)(R^2/R_0^2)_{\text{Av}}, \tag{2}$$

from that calculated by using the point-dipole assumption. R is the electron coordinate, a_0 and R_0 are the Bohr and nuclear radii, respectively, and Z is the nuclear charge. $(R^2/R_0^2)_{\text{Av}}$ is the density function of the nucleons that contribute to the magnetic moment. $R_0=1.5\times 10^{-13}A^{\frac{1}{3}}$ cm. For cesium, $Z=55$, and ϵ is of the order of 0.5%. Since the atomic wave functions in this region may be known, at best, only to a few percent, comparison with theory can be obtained only by considering the ratios of the hfs interactions in two isotopes, whereby the uncertainty in $|\psi(0)|^2$ is removed.[6,7] Thus, for the point-dipole theory, we obtain for the ratios

$$(\Delta\nu_1)_{\text{pd}}/(\Delta\nu_2)_{\text{pd}}=[g_1(2I_1+1)]/[g_2(2I_2+1)], \tag{3}$$

where $g=-\mu_I/I$; whereas if the finite extent of the nucleus is taken into account, the result is

$$(\Delta\nu_1)_{\text{ext}}/(\Delta\nu_2)_{\text{ext}}=\frac{(\Delta\nu_1)_{\text{pd}}}{(\Delta\nu_2)_{\text{pd}}}(1+\epsilon_1)/(1+\epsilon_2), \tag{4}$$

† This work was supported in part by the Army (Signal Corps), the Air Force (Office of Scientific Research, Air Research and Development Command), and the Navy (Office of Naval Research).

* Present address: Palmer Physical Laboratory, Princeton University, Princeton, New Jersey.

‡ Present address: Bell Telephone Laboratories, Murray Hill, New Jersey.

[1] F. Bitter, Phys. Rev. **75**, 1326 (1949).

[2] H. Kopfermann, *Kernmomente* (Akademische Verlagsgesellschaft, Leipzig, 1940), p. 17.

[3] A. Bohr and V. F. Weisskopf, Phys. Rev. **77**, 94 (1950).

[4] A. Bohr, Phys. Rev. **81**, 134 (1951); **81**, 331 (1951).

[5] E. Fermi, Z. Physik **60**, 320 (1930); E. Fermi and E. Segrè, Z. Physik **82**, 729 (1933).

[6] The volume effect of the charge distribution introduces a correction to the hfs interaction of the order of

$$(R_0Z/a_0)^{2(1-Z^2\alpha^2)^{\frac{1}{2}}-1},$$

where α is the fine structure constant.[7] For a pair of cesium isotopes differing by two neutrons, this would introduce an error in the cancellation of $|\psi(0)|^2$ of the order of 0.002%, which is an order of magnitude smaller than the measured effects. It should also be noted that perturbations by other Coulomb levels are negligible, since they are of the order of $\Delta\nu^2/\delta$, where δ is the distance of a perturbing level. In cesium the nearest is over 11 000 cm^{-1} away from the ground state. For one cesium isotope, this amounts to about 0.001% and is completely negligible in the ratio. The Crawford-Schawlow correction [Phys. Rev. **76**, 1310 (1949)] to the anomalies amounts to 0.01%, or less, but since it is in the same direction for all the isotopes, it cannot change the sign of Δ_{12}.

[7] H. B. G. Casimir, Arch. Musée Teyler, Ser. III, **VIII**, 201 (1936).

so that

$$\left[\frac{(\Delta\nu_1)_{\text{ext}}}{(\Delta\nu_2)_{\text{ext}}}-\frac{(\Delta\nu_1)_{\text{pd}}}{(\Delta\nu_2)_{\text{pd}}}\right]\Big/\frac{(\Delta\nu_1)_{\text{pd}}}{(\Delta\nu_2)_{\text{pd}}}\approx\epsilon_1-\epsilon_2. \quad (5)$$

This difference would be small compared with either ϵ_1 or ϵ_2 were it not that the distribution of nuclear magnetism was different for the two isotopes. The distribution is sensitive to the structure of the nucleus. In particular, Bohr and Weisskopf showed that the contributions to the anomaly are not identical for orbital and spin magnetizations. Consequently, different distributions of spin and orbital magnetizations for various models of the nucleus will lead to different anomalies. If one takes $(\Delta\nu_1)_{\text{ext}}/(\Delta\nu_2)_{\text{ext}}$ as the experimental ratio of the $\Delta\nu$'s, one obtains

$$[(\Delta\nu_1)/(\Delta\nu_2)]_{\text{exp}}\approx\{[g_1(2I_1+1)]/[g_2(2I_2+1)]\}\times(1+\epsilon_1-\epsilon_2), \quad (6)$$

or

$$\epsilon_2-\epsilon_1\equiv-\Delta_{12}=\{[g_1(2I_1+1)]/[g_2(2I_2+1)]\}\times[(\Delta\nu_2)/(\Delta\nu_1)]_{\text{exp}}-1. \quad (7)$$

The anomalies in some K, Rb, and Ag isotopes have been measured and comparison has been made with the theory. We have measured the hyperfine-structure anomalies in the four Cs isotopes, Cs^{133} (stable), Cs^{134} (2.3 years), Cs^{135} (3×10^6 years), and Cs^{137} (33 years). In the case of Cs^{133}, the nuclear moment[8] and hfs separation[9] had been measured with sufficient accuracy. However, for the radioactive isotopes, the measured values of $\Delta\nu$ were too inaccurate to uncover possible hfs anomalies, and the magnetic moments had not been measured. With this in mind we have made precision measurements of the hfs separations and nuclear g values of these isotopes, extending the atomic beam method used by Eisinger.[10]

II. THEORY OF THE EXPERIMENT

A. Energy Levels

The interaction Hamiltonian of an atom with a $J=1/2$ electronic ground state and nuclear spin I can be described by

$$H/h=a\mathbf{I}\cdot\mathbf{J}+\mu_0(g_J\mathbf{J}\cdot\mathbf{H}_C+g_I\mathbf{I}\cdot\mathbf{H}_C), \quad (8)$$

where H_C is an externally applied magnetic field, $a=\Delta\nu/(I+1/2)$, and g_I is expressed in Bohr magnetons. At zero field the separation between the two F-levels ($\mathbf{F}=\mathbf{I}+\mathbf{J}$) is $\Delta\nu$, each level being $(2F+1)$-fold degenerate. This degeneracy is removed with the application of H_C. The eigenvalues of (8) in an F, m_F representation, known as the Breit-Rabi equation[11] are given by

$$\frac{E(F,m_F)}{h}=\frac{-\Delta\nu}{2(2I+1)}+m_Fg_I\mu_0H_C\pm\frac{\Delta\nu}{2}\left(1+\frac{4m_Fx}{2I+1}+x^2\right)^{\frac{1}{2}}, \quad (9)$$

where $x=[(g_J-g_I)\mu_0H_c]/\Delta\nu$. The positive sign corresponds to $F=I+1/2$, the negative to $F=I-1/2$. The nuclear spin is 7/2 for Cs^{133}, Cs^{135}, and Cs^{137}, and is 4 for Cs^{134}. An energy-level diagram for spin 7/2 is given in Fig. 14; for spin 4, such a diagram is given by Eisinger, Bederson, and Feld[12] (hereafter referred to as EBF).

B. Atomic-Beam Method and Selection of Transitions

The experimental arrangement consists of a source of well-collimated atoms at one end of the apparatus, a detector at the other, and three magnets in the intervening region. The first (A magnet) has the gradient of its magnetic field in a direction transverse to the atomic beam; the second (C magnet) is homogeneous and contains a loop capable of introducing rf power into the system; and the third (B magnet) is also inhomogeneous. It is almost identical to the A magnet and has its gradient in the same direction. While it is in the field of an inhomogeneous magnet, the neutral atom experiences a transverse force component

$$F_z=-\mu_{\text{eff}}(\partial H_z/\partial z), \quad (10)$$

where

$$\mu_{\text{eff}}=\partial E/\partial H \quad (11)$$

is the effective magnetic moment. A plot of μ_{eff} for $J=1/2$, $I=7/2$ is given in Fig. 1.

Two methods were used to observe transitions. In the first, or flop-in method, the atom is required to undergo a change in the sign of μ_{eff} in the C magnet, in order to be refocused at the detector. In this case, an increase of detected atom counting rate is observed at resonance. In the second, or zero-moment flop-out method, the A- and B-fields must be selected so that in a given state the atom has $\mu_{\text{eff}}=0$ (see Fig. 1), and will be undeflected in passage through these fields. At resonance the atoms undergo a transition into a state for which $\mu_{\text{eff}}\neq0$ in the B magnet; hence they miss the detector with the result that a decrease of atoms is observed.[13]

In addition to the limitations imposed by the apparatus on possible transitions, the following quantum-mechanical selection rules apply (single quantum

[8] H. E. Walchli, Oak Ridge National Laboratory Report ORNL-1469, April 1, 1953 (unpublished), p. 50.
[9] L. Essen and J. V. L. Parry, Nature 176, 280 (1955).
[10] J. T. Eisinger, Ph.D. Thesis, Department of Physics, Massachusetts Institute of Technology, 1951 (unpublished).
[11] G. Breit and I. I. Rabi, Phys. Rev. 38, 2082 (1931).
[12] See, for example, Eisinger, Bederson, and Feld, Phys. Rev. 86, 73 (1952).
[13] Jaccarino, Bederson, and Stroke, Phys. Rev. 87, 676 (1952).

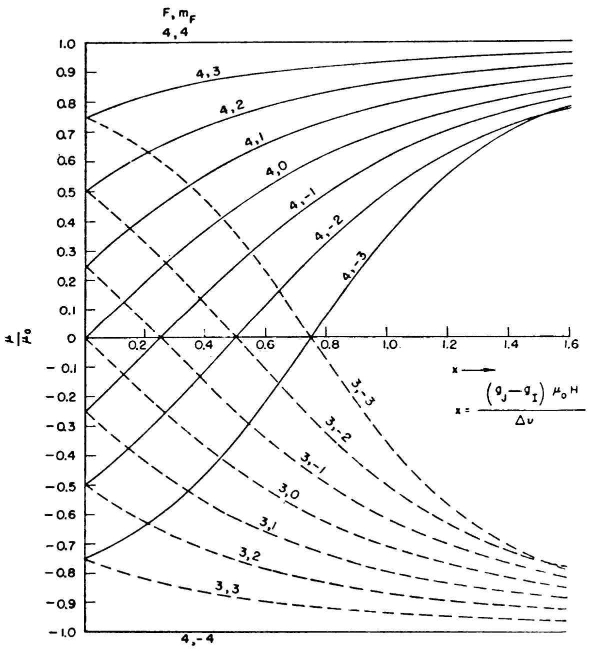

FIG. 1. Effective magnetic moments in an external magnetic field; $J=1/2$, $I=7/2$.

transitions were used):

$$\Delta m_F = \pm 1, \quad \Delta F = 0,$$
$$\Delta m_F = \pm 1, 0, \quad \Delta F = \pm 1. \qquad (12)$$

$\Delta m_F = 0$ transitions are excited by H_{rf} parallel to H_C (z-direction), while the others are excited by x and y components of the rf field.

The transitions used for finding $\Delta\nu$ are given in the Appendix. The selected transitions were both first-order field-independent lines ($m_F=0 \leftrightarrow m_F=0$ in the $I=7/2$ isotopes and $m_F=\pm 1/2 \leftrightarrow m_F=\mp 1/2$ in Cs^{134}), and adjacent transitions with "Zeemanicity" 1 (i.e., exhibiting a linear Zeeman effect equal to that of ν_z—see Appendix, Sec. A). The field-independent lines are not affected to first order by inhomogeneities in the C field, and are broadened only by the limited time Δt that the atom spends in the rf region (the broadening $\delta\nu$ is approximately $1/\Delta t$).[14] Measurements were made near zero-field.

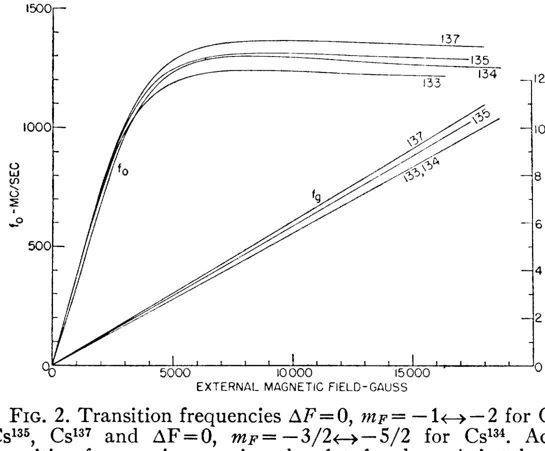

FIG. 2. Transition frequencies $\Delta F=0$, $m_F=-1 \leftrightarrow -2$ for Cs^{133}, Cs^{135}, Cs^{137} and $\Delta F=0$, $m_F=-3/2 \leftrightarrow -5/2$ for Cs^{134}. Actual transition frequencies are given by $f_0 \pm f_g$, where + is taken for the upper F level and − for the lower F level.

The measurement of g values, however, imposes stringent conditions on the selection of transitions. Pairs of lines exist whose frequency separation is $\nu_n \equiv 2g_I\mu_0 H_C$ (Appendix, Sec. A). Since this separation is small (e.g., for Cs^{133}, $\nu_n = 1.12$ kc/sec/gauss) and the line widths in the absence of field broadening are about 15 kc/sec, then the determination of the ratio of the g values for two isotopes to a precision of 1 part in 10^4 requires a field equal to or greater than approximately 10 000 gauss. If the magnetic field had a homogeneity of the order of 5 parts in 10^5 or better, the sole criterion would then be the satisfaction of the above condition. With the available magnet, however, unavoidable inhomogeneities in the C field broaden the lines considerably ($\delta\nu = (\partial\nu/\partial H_C)\Delta H_C$; note that $\Delta H_C/H_C \sim$ constant) unless H_C is selected so that $\partial\nu/\partial H_C$ is small. The most advantageous selection of the transition has to be made with the aid of Fig. 1. A transition is field independent when the initial and final states in a given field have the same μ_{eff}. Furthermore, with the requirement that the nuclear term be made as large as possible, it is seen that the conditions are satisfied by having μ_{eff} for the two states intersect at the maximum possible field. It is thus to be noted that $\Delta F=0$, $\Delta m_F = \pm 1$ transitions are preferable for two reasons: first, for the condition of equal μ_{eff}, ν_n is appreciably larger than for $\Delta F = \pm 1$ doublets; second, their μ_{eff} lines intersect at a smaller angle, which will make the transitions reasonably field-independent over a much greater range of fields than for $\Delta F = 1$ transitions. A plot of the transitions used is shown in Fig. 2; their field dependence, in Fig. 3. Actually, in Fig. 3 the g_I term in (9) is neglected, so that there is still a small field dependence $\pm g_I\mu_0$ to be added. A typical high-field resonance curve is shown in Fig. 4.

III. APPARATUS

The apparatus used for these experiments has been described as to vacuum system, magnets, and detector by EBF.[10,12,15] The following modifications were necessary: design of oven and techniques for handling the radioactive source; improvement of the mass spectrometer; and stabilization of rf sources and methods of observing transitions.

A. Oven and Material Handling

The oven was built specifically for handling radioactive atoms that are short lived for an apparatus

[14] The most probable velocity of the cesium atoms for 200°C temperatures is about 3×10^4 cm/sec. With the assumption that the rf extends one-half of a gap width outside of the actual flop wire, a 15-kc/sec rf width is obtained for the 1.6-cm wire.

[15] The original design of the apparatus was by Dr. Hin Lew.

with conventional surface ionization detection. The necessity of utilizing a maximum of the source atoms requires a channel oven. It can be shown[16] that the ratio of the number of atoms emerging from a thin wall oven that has slit diameter d to the number emerging from a channel oven that has channels of length L and diameter d is of the order of L/d. It is assumed that the vapor pressure of the material in the oven is low enough so that the mean free path is much greater than L. The number of atoms in a very small solid angle in the forward direction is the same in both cases and is determined solely by the aperture of the oven. It is the number of atoms emerging at the larger angles (these atoms are not useful for the experiment) that is cut down by the directional oven in such a manner that the ratio of intensities integrated over all directions is reduced by the factor L/d, which was 50 in our case. The slits consist of nine No. 26 gauge hypodermic

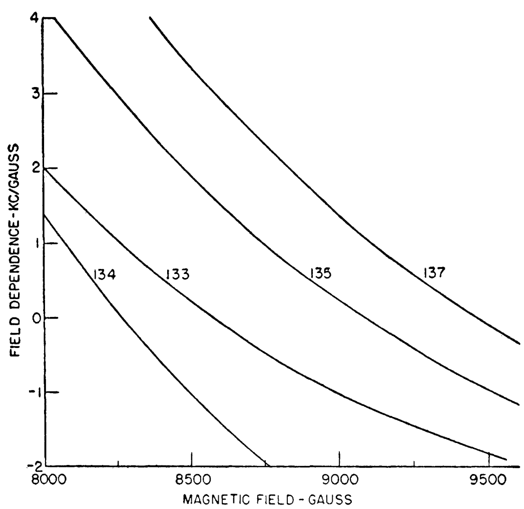

FIG. 3. Field dependence of transitions used for g-value measurements.

needles cut to 1/2-in. lengths and silver-soldered into the holder. The hypodermics were flattened on two sides as shown in Fig. 5, so that 56% of the total slit area was open to the beam. A schematic scale drawing of the oven is shown in Fig. 5.[17] The oven block, plug, and slit holder are made of monel. It was heated by by nine molybdenum wire coils insulated from the block by thin quartz tubing. The sample was actually loaded into a monel cup that was 3/16 in. o.d. and 0.150 in. high. A lip on the top provided for its insertion into the oven well by means of bent-out tweezers. The use of the cup was required to permit thorough evaporation of the sample solvent. A set of baffles

[16] P. Clausing, Physica **9**, 65 (1929); L. Davis, Jr., Research Laboratory of Electronics, Massachusetts Institute of Technology, Technical Report 88, December 1, 1948 (unpublished).

[17] Much of the oven design was by Mr. F. J. O'Brien of the Research Laboratory of Electronics, Massachusetts Institute of Technology.

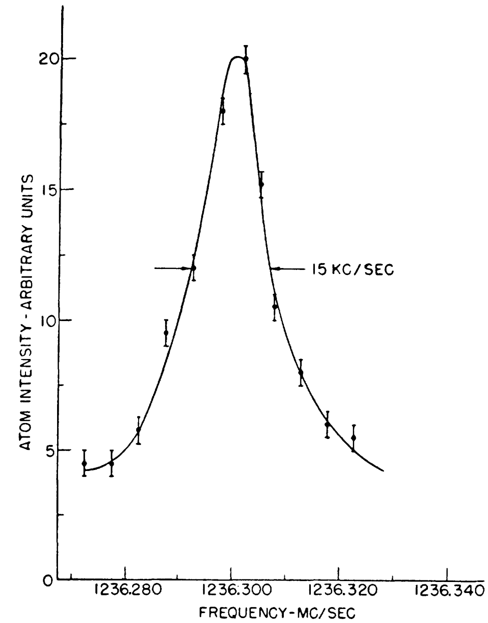

FIG. 4. Cs^{133} g-value resonance curve.

was screwed into the bottom of the plug to prevent "Spritz" (not shown in Fig. 5) as suggested by Eisinger and Bederson.[18] An iron-constantan thermocouple was screwed to the oven block to measure the temperature, which was usually maintained at about 200°C.

The radioactive samples were obtained as CsCl in a weak HCl water solution from Oak Ridge National

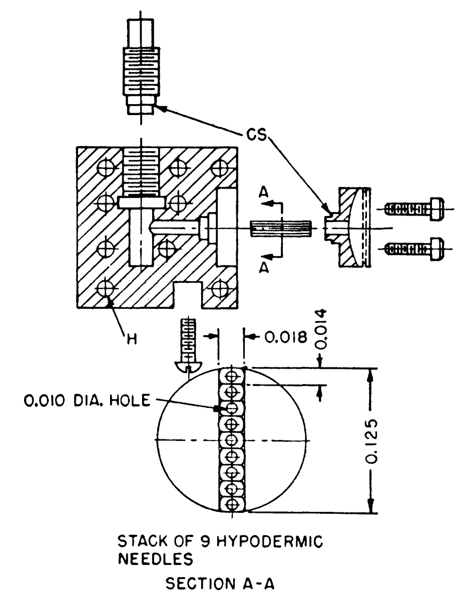

FIG. 5. The atom oven. CS are plated copper seals, H are heating coils.

[18] J. T. Eisinger and B. Bederson, Research Laboratory of Electronics, Massachusetts Institute of Technology Technical Report 212, January 28, 1952 (unpublished).

Laboratories. This form permits easier and more controlled transfer of the material into the oven than does the previously used hygroscopic Cs_2CO_3 powder.[13] Na_2CO_3 was used to neutralize the HCl, and, after thorough evaporation, freshly-cut K metal was added, as well as stable CsCl. For the g-value runs, 150 millicuries of Cs^{134} and 15 millicuries of $Cs^{135}-Cs^{137}$ were used and half as much was used for the $\Delta\nu$ runs. It should be noted that with isotopes that are relatively long lived, decontamination presents numerous problems.

B. Magnetic and rf Fields

The deflecting magnets, as described by EBF, were modified only by providing a trimming current for the B field to optimize zero-moment intensities (see Fig. 6).

The C magnet (0.246 gap width) in addition to its main windings has an auxiliary set of low-current trimming windings useful for near zero-field $\Delta\nu$ experiments. The homogeneity of the magnet over the rf region is better than 0.03%. This was shown by the lack of appreciable field broadening of the high-field transitions.

Copper-strip hair-pin type rf flop wires, 1 cm and 1.6 cm long, were used. In addition to the collimators shown by EBF, a stopping ribbon[19] was used to reduce undesirable background.

C. Detection and Mass Spectrometry

A surface ionization tungsten ribbon 0.010 in. wide was used as the detector. The Cs^+ ion beam was analyzed with a 60° mass spectrometer magnet, and its intensity measured either with a FP 54 electrometer-galvanometer system (over-all sensitivity 5×10^{-17} amp/mm) in the case of Cs^{133}, or counted with a beryllium-copper electron multiplier,[20] for the low intensities of the radioactive isotopes. Cs^{133} beams of the order of 3000 mm were obtained at the operating temperature, and the approximate relative intensities of the radioactive isotopes are shown in Fig. 7. For example, in the case of $Cs^{134}\Delta\nu$ measurements, a counting rate of 50 atoms per second was observed at resonance.

Good mass-spectrometer resolution was essential, since the abundance of radio-isotopes was small compared with that of Cs^{133}. Initial unreproducible results and poor resolution were traced to charge deposits on dielectric surfaces (pump oil films) along the path of the analyzed ion beam. To remedy this, a closed grounded guide was made to completely shield the ion beam and it was kept oil-free by continuous heating to approximately 150°C.[21] The resolution was raised thereby from as low as 3 to better than 5000 for $Cs^{133}-Cs^{134}$.[22] A composite mass spectrometer resolution curve, obtained by combining the curves of Cs^{134} and $Cs^{135}-Cs^{137}$,[23] is shown in Fig. 7.

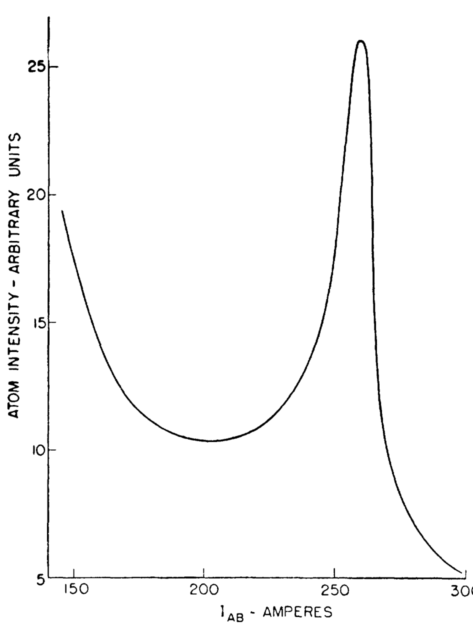

FIG. 6. Plot of second zero-moment in Cs^{133}. Slit width, approximately 0.007 in.; gradient-field ratio, 1.57/cm; magnet length, 25 in.

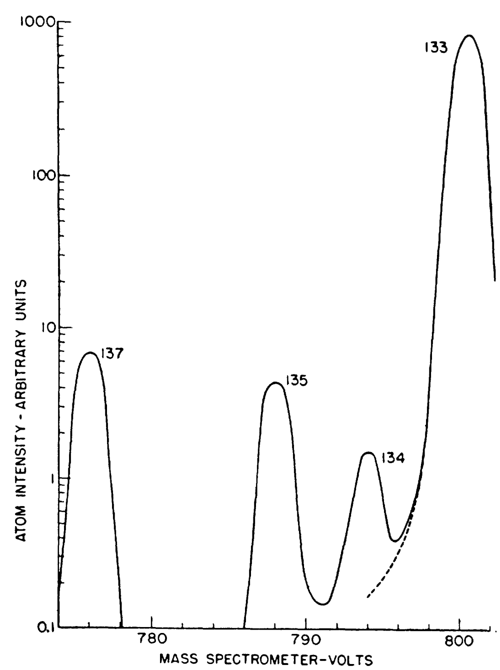

FIG. 7. Mass spectrometer resolution curves.

[19] J. R. Zacharias, Phys. Rev. **61**, 270 (1942).

[20] H. Lew, Phys. Rev. **76**, 1086 (1949).

[21] Bederson, Eisinger, and Jaccarino (private communication).

[22] We define the resolution as the inverse fraction of the number of atoms of type A detected at the A' mass spectrometer setting.

[23] Cs^{135} and Cs^{137}, obtained from fission fragments, are always found together in the sample with the relative abundances shown. This seems to agree with the fission-yield findings of Fleming, Tomlinson, and Thode, Can. J. Phys. **32**, 522 (1954).

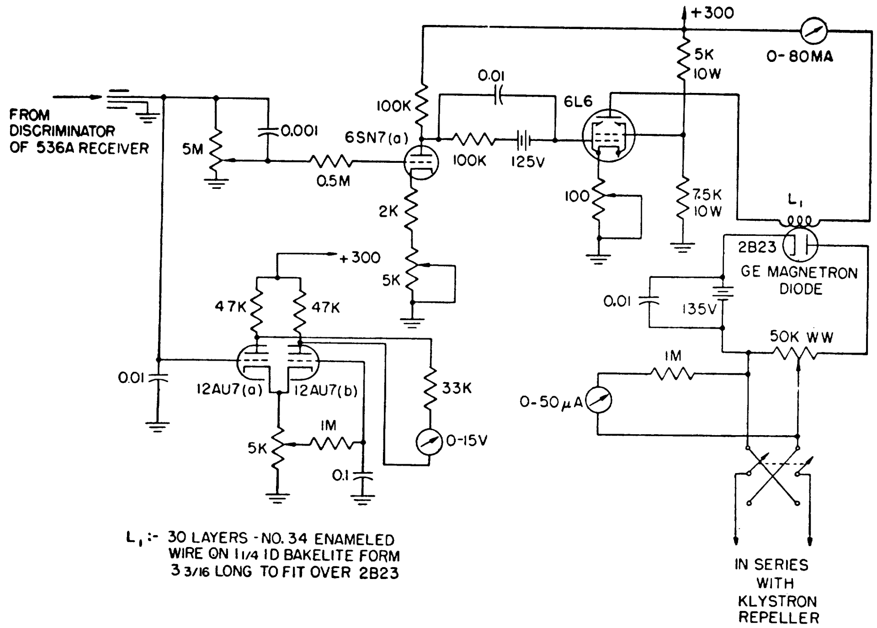

FIG. 8. Klystron stabilizer circuit.

D. Frequency Systems

The $\Delta\nu$ frequencies were in the range of 9000–11 000 Mc/sec. Since the expected line widths were of the order of 15 kc/sec, considerable care was required in the operation of the Varian type X-13 klystron used to generate these frequencies. Filament and repeller voltages were obtained from batteries, and the tube was shock mounted. In addition, cooling was accomplished by attaching to the klystron conducting fins whose ends were dipped in dry ice. This considerably improved the noise figure by eliminating the noise introduced mechanically by forced air cooling. Nevertheless, to obtain the requisite stability and to permit controlled scanning of the lines, stabilization of the klystron was required. The stabilizer circuit is shown in Fig. 8; a complete block diagram of the rf system in Fig. 9.[24] The resultant short-time stability was found to be of the order of 100 cps. An extremely clean and fairly strong harmonic signal from the crystal standard was required, this being achieved by multiplying to 450 or 480 Mc/sec in tubes. Further multiplication was then accomplished in crystals to obtain frequencies sufficiently near the $\Delta\nu$'s so that the beat between these standard frequencies and the klystron could be conveniently received on the S-36 receivers. Coarse frequency measurements (to about 0.01%) were first made with a Hewlett-Packard X530A absorption cavity wave meter. The standard 5-Mc/sec crystal was kept to within better than 1 cps of the WWV signal. Precise frequency measurement was then made by zero-beating the General Radio 805 signal generator with the beat between the klystron and the standard in the S-36 AM receiver and then measuring the G.R. 805 frequency with the H.-P. 524 A frequency counter.

The transition frequencies of the g-value measurements were in the range of 1200 to 1400 Mc/sec. They were generated by 707 B reflex klystrons with tunable external cavities. All voltages were obtained from batteries, and the tubes were shock-mounted; forced air cooling was not required. Under these conditions, the klystrons were found to be inherently sufficiently stable. Probes were inserted into the cavities for frequency-measuring purposes. For reasons described in the following section, the doublet frequencies generated by two separate klystrons were fed simultaneously into one flop wire. With adequate decoupling, pulling of one klystron by the other was eliminated. The individual frequencies could be measured by closing switches 1 and 2 in Fig. 10. The TSF 6TX cavity wave meter and the Cardwell TS-175/U frequency meter gave the rough frequencies; the crystal standard and the G. R. 805 interpolation oscillator, measured with the H.-P. frequency counter, gave the more precise values. In most of the actual runs, only the difference frequency of the two klystrons (about 10 Mc/sec) had to be measured. This was accomplished directly by beating the difference signal with the G. R. 805 oscillator and measuring it with the H.-P. counter. The internal crystal of the counter was monitored with WWV.

IV. EXPERIMENTS AND RESULTS

A. $\Delta\nu$ Transitions

Predictions for the values of $\Delta\nu$ were available from low-frequency data[25–27,13] (see Table I) to within ± 15

[24] The use of the 2B23 circuit in making the transition to repeller potential was suggested by Dr. C. A. Lee of Columbia University.

[25] E. H. Bellamy and K. F. Smith, Phil. Mag. 44, 33 (1953).
[26] Davis, Nagle, and Zacharias, Phys. Rev. 76, 1068 (1949).
[27] L. Davis, Phys. Rev. 76, 435 (1949).

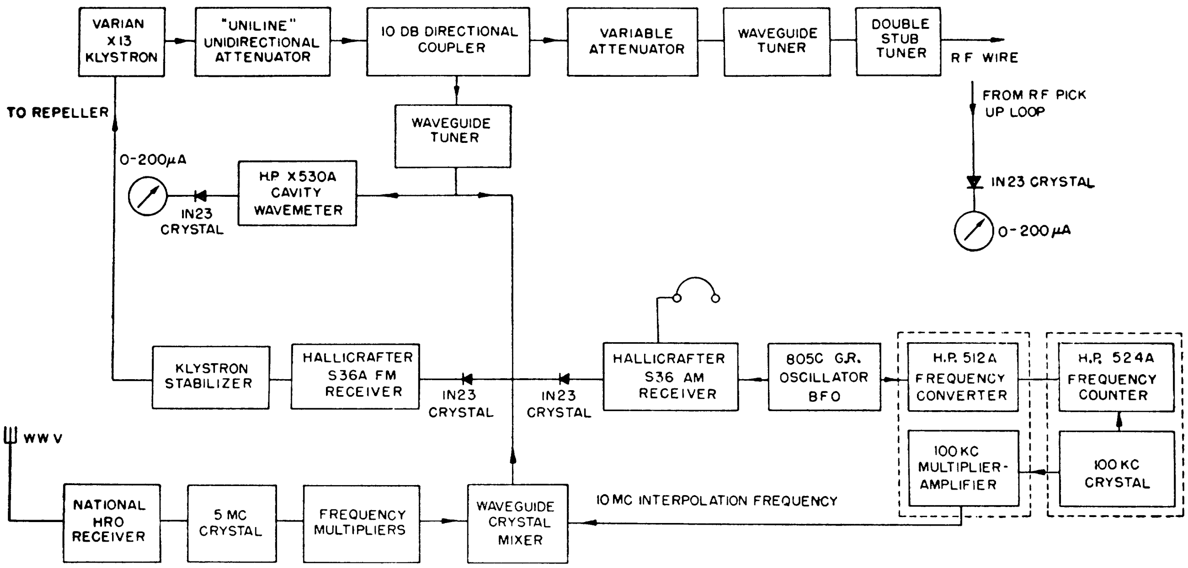

FIG. 9. $\Delta\nu$ frequency system.

Mc/sec. The C field was set as low as possible in order to avoid large corrections to the measured values of the transition frequencies in obtaining $\Delta\nu$. The field, however, had to be maintained above approximately 1 gauss in order to avoid "Majorana" flop. The FM receiver in the klystron stabilizing feedback loop operated in the range of 28 to 46 Mc/sec. Since this range determined the required difference beat between the frequencies of the klystron and the crystal harmonics of the standard, appropriate standard frequencies had to be used to cover the predicted range of $\Delta\nu\pm$ 15 Mc/sec. These conditions were satisfactory in the case of Cs^{134} and Cs^{135} in which the $\Delta\nu$'s were found within the predicted values. With Cs^{137} this was not the case, and it was found advantageous to keep the range of frequency search constant and to use a small C field in order to increase the Zeeman frequency and thus bring one of the field-dependent lines into the frequency range under observation. The identification of a given transition was made by observing its field dependence as compared with that of a low-frequency Zeeman line, ν_z. A typical resonance curve is shown in Fig. 11. Once the lines were identified and ν_z was known, it was possible to search for the first-order field-independent lines. In the case of the spin 7/2 isotopes, these are the $0\leftrightarrow 0$ transitions. These $\Delta m_F=0$ transitions suffered a symmetrical peak Doppler splitting, the peaks being listed under ν_+ and ν_- in Table VIII of the Appendix, Sec. B. In the case of Cs^{134}, the field-independent lines are $\Delta m_F=\pm 1$; they were found to be single, as expected (Fig. 12). First, resonance curves were obtained, and later the peaks were determined; the average of several values are given in Table VIII. The weighted averages of the results are given in Table I. Both statistical and systematic errors, such as possible small deviations of the crystal from the WWV frequency, are included in the quoted error. These procedures were used with Cs^{135} and Cs^{137}. With Cs^{134} a $-5\nu_z$ high-frequency transition was first identified, followed by a $-1\nu_z$ high-frequency transition. The z-component wire, in which the low-frequency transitions could not be easily observed, was used for both observations. Thus for runs 1 and 2 of Table VIII, ν_z is extrapolated from two adjacent xy-wire measurements. These runs were not used in arriving at the

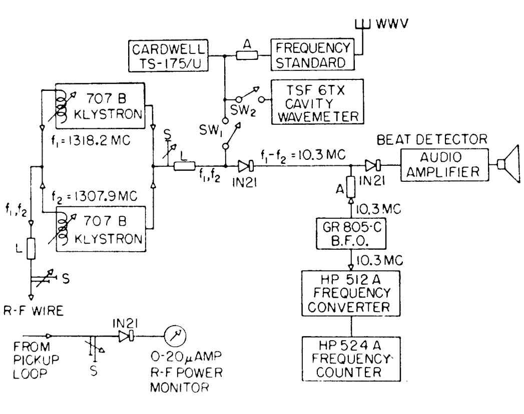

FIG. 10. g-value frequency system.

TABLE I. $\Delta\nu$ weighted averages.

Isotope	$\Delta\nu$—Direct transitions Mc/sec present work	$\Delta\nu$—Low-frequency data Mc/sec
Cs^{134}	10 473.626±0.015	10 465 ±12[13]
		10 440 ±30[25]
Cs^{135}	9 724.023±0.015	9 724 ± 8[26]
Cs^{137}	10 115.527±0.015	10 126.5± 7[26]
		10 128 ±15[27]

weighted average value but served only to find the field-independent lines.

B. Measurements of the g Values

The g values were obtained from the doublet transitions, Eq. (28), Appendix, Sec. A. Actually, instead of measuring H_C directly, a similar doublet was measured in another isotope, thereby yielding g-value ratios. The experiments were carried out in fields of the order of 9000 gauss, with magnet currents of approximately 400 amp. Since there was a field drift of some 0.01% per minute, it was essential that the measurements be made rapidly and repeatedly, alternating the two isotopes so that the doublet frequencies for both could be extrapolated to a common time. This procedure is illustrated in Fig. 13. Preliminary data for the stable isotope obtained by using a 6-cm rf wire showed con-

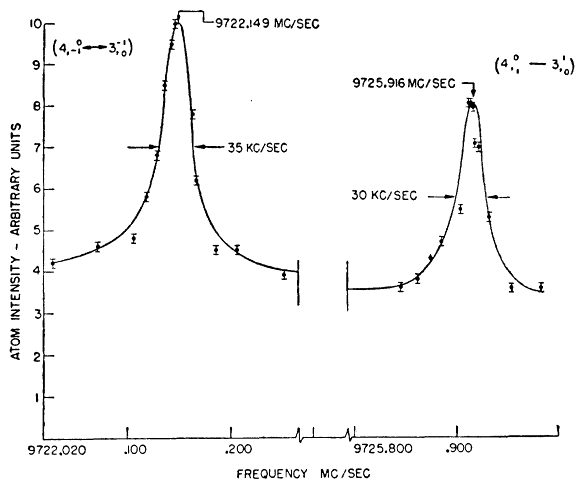

FIG. 11. Cs^{135} $\Delta\nu$ resonance curve.

siderable structure that varied with the type of rf feeding and matching of the re-entrant wire. In a shorter wire, a single symmetrical peak could be obtained, as shown in Fig. 4, once the rf power was properly adjusted. The structure observed in the larger wire was apparently caused by the combination of asymmetric rf field distribution and inhomogeneities of the dc field.[28]

The doublet separation varies linearly with time; the individual frequencies do not. Therefore, both transitions of a doublet were observed simultaneously, and their joint maximum[29] was determined. In addition, this procedure saved time and increased the over-all signal-to-noise ratio, which was advantageous at the

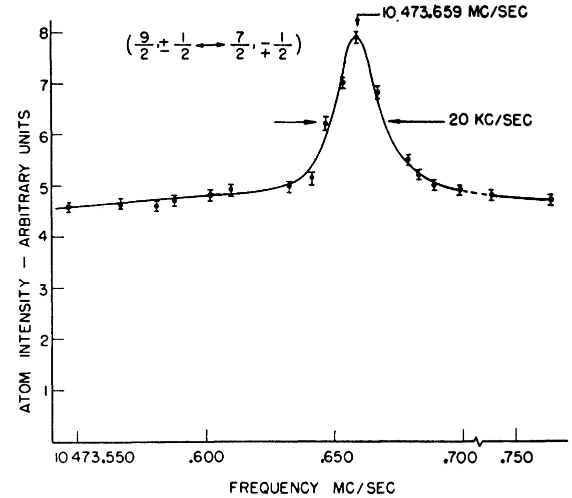

FIG. 12. Cs^{134} $\Delta\nu$ resonance curve.

low counting rates used. A check on the method was obtained by making a run in which the individual frequencies were measured; these results are given in Table IX. A long running-time was required for these initial runs because only two oscillators were used, so that the cavities had to be retuned at every change of isotope. For the later runs, two more oscillators were built, which required only slight retuning to compensate for the field drift. It was possible to select A and B fields so that transitions in both isotopes were observable with the same setting. This avoided varying corrections arising from small stray fields that might reach the rf region. The Cs^{133}, Cs^{135}, and Cs^{137} transitions (these isotopes have identical spins and $\Delta\nu$'s within $\sim$10% of each other) could thus be observed as flop-in, but in the case of Cs^{134}, the proper A- and B-field setting for Cs^{134} flop-in corresponded to the second zero moment in Cs^{133}, so that the latter was observed as a zero-moment flop-out.

The line transition frequencies were approximately 1241 ± 5 Mc/sec for Cs^{133}; 1313 ± 5 Mc/sec for Cs^{135}; 1366 ± 6 Mc/sec for Cs^{137}; and 1301.5 ± 5 Mc/sec for Cs^{134}. By making rf impedance measurements on the flop wire in the C field over this frequency range, no

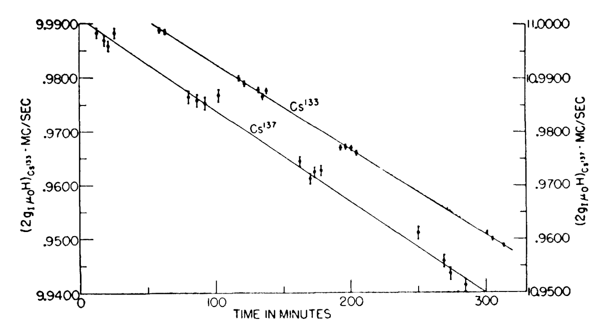

FIG. 13. Time-drift plot of Cs^{133} and Cs^{137} doublet frequency separations; approximate field, 9000 gauss.

[28] N. F. Ramsey (private communication).

[29] N. F. Ramsey (Atomic Beam Conference, Brookhaven National Laboratory, Aug. 17–19, 1954) calculated that feeding two frequencies ω_1 and ω_2 into one flop wire will produce a shift in resonance frequency of the order of $\Delta\omega=2b^2/(\omega_1-\omega_2)$, where b is the line width. In the present experiment, this amounts to about 0.05 kc/sec, which is negligible.

TABLE II. g-value ratios, weighted averages. The indicated error limits are standard deviations.

Isotopes	g-value ratio
Cs^{135}/Cs^{133}	1.05820 ± 0.00008
Cs^{137}/Cs^{135}	1.04005 ± 0.00008
Cs^{137}/Cs^{133}	
Calculated from first two ratios	1.10058 ± 0.00013
Measured	1.10037 ± 0.00015
Cs^{134}/Cs^{133}	1.01447 ± 0.00029

peculiar rf resonances were observed.[30] We noted (see Fig. 4) that a resonance in Cs^{133} exhibited a symmetrical curve. This justified our making only peak determinations in the resonances of the radio-isotopes. Care was taken to optimize rf power in each case. From Fig. 3, it can be seen that the least-field dependence in the lines can be achieved only for adjacent pairs of isotopes (i.e., Cs^{133}–Cs^{134}, Cs^{133}–Cs^{135}, and Cs^{135}–Cs^{137}). Thus in the case of the Cs^{133}–Cs^{137} runs, performed for an internal consistency check, a simultaneous optimum C field for both isotopes could not be selected and somewhat greater errors resulted. For Cs^{134} the greater uncertainty is the result of the relatively poorer counting rate. The data for each pair of isotopes were plotted as a function of time (Fig. 13). A least-square-fit straight line was calculated for the isotope of a given pair on which most of the measurements were made. From the ratio of the $\Delta\nu$'s, the slope of a corresponding line for the other isotope could be calculated (neglecting here the small Bohr-Weisskopf effect). The ratio of the g values and the standard deviations were then calculated at a given central time. In two instances the field variation was not linear, and curves giving the best fit had to be drawn. The weighted averages for the g-value ratios are given in Table II. The experimental data of the runs are given in the Appendix, Sec. B, Tables X to XIII.

C. Magnetic Moments

The magnetic moment of Cs^{133} as measured by nuclear resonance technique is $+2.57893$ nm.[8] This value includes the magnetic-shielding correction which makes the measured magnetic moment appear smaller by a factor $1-\sigma=0.99427$ for $Z=55$, where σ is the magnetic-shielding constant.[31] The correction has an estimated accuracy of 5%. The magnetic moments calculated from this value and the ratios of Table II are given in Table III.

D. Hyperfine-Structure Anomalies

From Eq. (7), we obtain the hfs anomalies given in Table IV, using the values listed in Tables I and II and the value $\Delta\nu=9192.631830\pm0.0000010$ Mc/sec for Cs^{133}, which was already known.[9] These results are compared with the theory in the following section.

V. INTERPRETATION AND DISCUSSION OF RESULTS

A. Theory

A qualitative estimate of the hfs anomalies was given in Sec. I. Bohr and Weisskopf[3] calculated this effect by considering the valence electron's interaction with a distributed nuclear magnetic moment. This distribution they assumed to be spherically symmetric and made up of separate spin and orbital contributions. They took into account the variation of the radial electron wave function inside a uniform distribution of nuclear charge. They found a departure from $\Delta\nu$ obtained in (1), given by

$$\epsilon=-(\kappa_s)_{\mathrm{Av}}\alpha_s-(\kappa_l)_{\mathrm{Av}}\alpha_l. \tag{13}$$

Here the α_i are fractional contributions of spin and orbit to the total nuclear moment, and the κ_i are the relative decreases of these contributions to $\Delta\nu$ as a consequence of the deviation of the nuclear magnetization from a point dipole. The κ_i are given by Eq. (18) of reference 3 as $(\kappa_s)_{\mathrm{Av}}=b(R^2/R_0^2)_{\mathrm{Av}}$, and $(\kappa_l)_{\mathrm{Av}}=0.62\times b(R^2/R_0^2)_{\mathrm{Av}}$. The parameter b, which is a function of Z and $R_0=1.5\times10^{-13}\ A^{\frac{1}{3}}$ cm, is also tabulated.[3] For cesium, $b=1.37\%$. Combining this with (13), we have

$$\epsilon=-(\alpha_s+0.62\alpha_l)b(R^2/R_0^2)_{\mathrm{Av}}. \tag{14}$$

Bohr[4] notes that, in a single-particle model, it is not a good assumption to neglect the angular asymmetries of the nuclear moment distribution in the calculation of the κ_s, as was done in reference 3. Consideration of these asymmetries modifies κ_s by a factor $(1+0.38\zeta)$, where

$$\zeta=(2I-1)/4(I+1) \text{ for } I=l+1/2,$$
$$\zeta=(2I+3)/4I \quad\text{ for } I=l-1/2. \tag{15}$$

Equation (14) then becomes

$$\epsilon=-[\alpha_s(1+0.38\zeta)+0.62\alpha_l]b(R^2/R_0^2)_{\mathrm{Av}}. \tag{16}$$

The calculation of the anomalies requires knowledge of $(R^2/R_0^2)_{\mathrm{Av}}$ as well as a knowledge of the relative spin and orbital contributions to the magnetic moment.

TABLE III. Magnetic moments.

Isotope	Spin	Odd-nucleon state Proton	Neutron	g_{exp}	μ nuclear magnetons uncorrected	μ nuclear magnetons with diamagnetic correction
Cs^{133}	7/2	$g_{7/2}$		0.737	$+2.564221\pm0.000028$	$+2.57893\pm0.00003$[8]
Cs^{134}	4	$g_{7/2}$	$d_{3/2}$	0.747	$+2.9729\pm0.0009$	$+2.9900$
Cs^{135}	7/2	$g_{7/2}$		0.780	$+2.7134\pm0.0003$	$+2.7290$
Cs^{137}	7/2	$g_{7/2}$		0.811	$+2.8219\pm0.0003$	$+2.8382$

[30] This procedure was suggested by Professor R. H. Dicke, of Princeton University.
[31] E. Segrè, *Experimental Nuclear Physics* (John Wiley and Sons, Inc., New York, 1953), Vol I, p. 443.

The value $1.5\times10^{-13}A^{\frac{1}{3}}$, used for R_0 may be high in view of recent indications. This may change the absolute values of the ϵ_i, but it enters only as a scale factor when comparing sets of isotopes. The value of the single-particle density function should lie approximately between 3/5 and 1, which are the values for a uniform and surface distribution. Bohr,[4] however, gives an estimate of the variation of $(R^2/R_0^2)_{\text{Av}}$ with the particle angular momentum. The results are 0.49, 0.66, 0.80 for the proton in p, d, f orbits, and 0.85 for a neutron in an f orbit. For the $g_{7/2}$ proton and $d_{\frac{3}{2}}$ neutron in Cs^{134}, Bohr[32] indicates that 0.90 and 0.70 are good extrapolations. The smaller neutron well depth, which allows more of the neutron wavefunction to lie outside R_0, accounts for the difference in proton and neutron values of $(R^2/R_0^2)_{\text{Av}}$ for the same angular momentum.

B. Calculation of Anomalies and Comparison with Experiment

Models 1(a) and 1(b)

The theory of Bohr and Weisskopf is applied to the four nuclei; Eq. (14) is used and an extreme single-particle model is assumed. We have

$$g=\left(\frac{\mathbf{S}\cdot\mathbf{I}}{I(I+1)}\right)g_s+\left(\frac{\mathbf{L}\cdot\mathbf{I}}{I(I+1)}\right)g_l, \tag{17}$$

where $\mathbf{I}=\mathbf{L}+\mathbf{S}$ for the nucleon. The orbits of the nucleons are obtained from shell theory.[33] The terms on the right-hand side of (17) yield α_s and α_l, when divided by g. If we use $g_l=1$ and $g_s=5.6$ for the proton, and $g_l=0$ and $g_s=-3.8$ for the neutron, we obtain the familiar Schmidt limits for the magnetic moments. In order to account for the difference between the Schmidt-limit value and the experimental g value (given in Table III) two possibilities were proposed.

Model 1(a)

The difference between g_{exp} and g_{Schmidt} can be eliminated by a reduction of the value of the intrinsic moment of the odd nucleon[34] used in (17). This reduction is considered to be caused by exchange currents in the nucleus. We find that $g_s^{\text{eff}}=10-9g$. This yields 3.37, 2.98, and 2.70 for Cs^{133}, Cs^{135}, and Cs^{137}, respectively. Then α_s becomes -0.51, -0.42, and -0.37 for the three isotopes. In the case of Cs^{134}, the angular momenta of the two odd nucleons add to yield the total nuclear spin I. We find that

$$g=\frac{\mathbf{I}_p\cdot\mathbf{I}}{I(I+1)}g_p+\frac{\mathbf{I}_n\cdot\mathbf{I}}{I(I+1)}g_n. \tag{18}$$

[32] A. Bohr (private communication).
[33] M. G. Mayer and S. A. Moszkowski, Revs. Modern Phys. **23**, 315 (1951); L. A. Nordheim, Revs. Modern Phys. **23**, 322 (1951).
[34] F. Bloch, Phys. Rev. **83**, 839 (1951); H. Miyazawa, Repts. Progr. in Phys. **6**, 263 (1951).

TABLE IV. Hyperfine-structure anomalies—experimental values.

Isotopes 1	Isotopes 2	$-\Delta_{12}$ percent
Cs^{135}	Cs^{133}	$+0.037\pm0.009$
Cs^{137}	Cs^{133}	$+0.009\pm0.010$
Cs^{137}	Cs^{135}	-0.020 ± 0.009
Cs^{134}	Cs^{133}	$+0.169\pm0.030$

In (18) it is assumed that the state of the odd proton is not affected by the addition of the odd neutron, so that for g_p we use $g_{\text{exp}}(Cs^{133})$. With $I_p=7/2$ and $I_n=3/2$ we obtain, from (18), $g_n=0.785$. From (17), letting $I=I_n$, $g_l=0$, and using the above value of g_n, we find, for the effective intrinsic value of the neutron moment,

$$g_{ns}^{\text{eff}}=-5g_n=-3.93.$$

Using these values in (18), we obtain $g=\frac{4}{5}g_p+\frac{1}{5}g_n$, $\alpha_{sp}=\frac{4}{5}\alpha_s=-0.41$, $\alpha_{lp}=\frac{4}{5}\ \alpha_l=1.21$, and $\alpha_{sn}=(-1/25)\times(g_s^{\text{eff}}/g)=0.21$). The values previously found for Cs^{133} are inserted for α_s and α_l. The total anomaly is obtained by summing the ϵ's arising from the proton and the neutron.

Model 1(b)

We assume g_l instead of g_s to be modified by the exchange currents,[12] so as to yield g_{exp} from (17). We obtain from (17) and (18) $g_l^{\text{eff}}=1.22$, 1.26, 1.29, and $\alpha_s=-0.84$, -0.80, -0.77 for Cs^{133}, Cs^{135}, and Cs^{137}, respectively. Then for Cs^{134}, $\alpha_{sp}=-0.67$, $\alpha_{lp}=1.47$, $g_{ln}^{\text{eff}}=0.02$, $\alpha_{sn}=0.19$, $\alpha_{ln}=0.01$, where we have used for g_{sp} and g_{sn} their free moment values 5.6 and -3.8. The results are given in Table V.

Models 2(a) and 2(b)

Equation (16) is applied to the four nuclei. Model 2(a) uses an effective g_s and Model 2(b) an effective g_l. For the $g_{7/2}$ proton in the spin 7/2 isotopes, $I=l-1/2$ so that, from (15), we have $\zeta=5/7$. In the case of Cs^{134} we must again consider the neutron and proton contributions separately. For the $d_{3/2}$ neutron, $l=2$, $I=l-1/2$, and $\zeta=1$. Equation (16) yields

$$-\epsilon=[(1+0.38\times5/7)\alpha_{sp}+0.62\alpha_{lp}](1.37)(0.90)+(1+0.38)\alpha_{sn}(1.37)(0.70),$$

in which we have used the indicated values of b and $(R^2/R_0^2)_{\text{Av}}$. Since it will be of interest later, we also calculate $\epsilon(Cs^{134})$, assuming the ground state of the nucleus to be a mixed configuration of $d_{5/2}$ and $g_{7/2}$ protons. The mixture is adjusted so as to give the experimental g-value where g_s^{free} is used and we take $g_l=1$ for the proton and $g_l=0$ for the neutron. A mixture of 80% $g_{7/2}$ state and 20% $d_{5/2}$ state is obtained, and this proportion is also used in the calculation of ϵ.

Model 3

Bohr[4] considers another model in which the single-particle magnetic moment is coupled to the moment of

TABLE V. hfs anomalies—comparison with theory. Models: 1(a) Bohr-Weisskopf theory $g_{lp}=1$; $g_{ln}=0$, g_s^{eff}; 1(b) Bohr-Weisskopf theory g_l^{eff} g_s^{free}; 2(a) A. Bohr, single-particle theory, $g_{lp}=1$, $g_{ln}=0$, g_s^{eff}; 2(b) A. Bohr, single-particle theory, g_l^{eff}, g_s^{free}; 3 A. Bohr, asymmetric core model; 4 Feenberg-Davidson model.

Isotope	Δ (exp) %	1(a) ε%	1(a) Δ%	1(b) ε%	1(b) Δ%	2(a) ε%	2(a) Δ%	2(b) ε%	2(b) Δ%	3 ε%	3 Δ%	4 ε%	4 Δ%
Cs^{134}		−0.620		−0.488		−0.560[a]		−0.380					
	+0.169 ± 0.030		+0.094		+0.118		+0.205[a]		+0.293				
Cs^{133}		−0.526		−0.370		−0.355		−0.087		−0.422		−0.212	
	+0.037 ± 0.009		+0.040		+0.024		+0.072		+0.035		+0.053		+0.085
Cs^{135}		−0.567		−0.394		−0.427		−0.122		−0.475		−0.297	
	−0.020 ± 0.009		+0.024		+0.013		+0.040		+0.023		+0.019		+0.063
Cs^{137}		−0.591		−0.407		−0.467		−0.145		−0.494		−0.360	

[a] A Cs^{134} $d_{5/2}-g_{7/2}$ mixed configurations with g_s^{free} gives $\epsilon=-0.468\%$ and $\Delta=+0.113\%$.

an asymmetric rotating core. If we assume that the coupling scheme is intermediate between very strong spin-orbit coupling and a spin-orbit coupling smaller than the coupling of l to the nuclear axis, though still involving a larger energy than the nuclear rotational level spacing, we have, for the angular asymmetry parameter

$$\zeta=\frac{2I-1}{4(I+1)};\quad I=l+\tfrac{1}{2},$$

$$\zeta=\frac{1}{4(I+2)}\frac{1}{\beta^2-1}(\beta^2(2I+1)-6\beta(2I+1)^{\frac{1}{2}}+5-2I);\quad I=l-\tfrac{1}{2},\qquad(19)$$

where β depends on the strength of the ls coupling as compared with the coupling between l and the nuclear axis. For this coupling scheme, the total angular momentum of the single particle has a constant Ω (assumed equal to I) along the nuclear axis.

The g factor associated with Ω is given by

$$Ig_\Omega=\sigma g_s+(I-\sigma)g_l,\qquad(20)$$

where σ is the average odd-particle spin component on the nuclear axis. A simple vector model (see Fig. 2 of Blin-Stoyle[35]) shows that this quantity is given by

$$\sigma=\frac{(I+1)g-g_R-Ig_l}{g_s-g_l},\qquad(21)$$

in which g is the experimental g value, $g_s=g_s^{\text{free}}$, $g_l=1$, and g_R is the core g-value, which is expected to be of the order of Z/A or approximately 1/2 for cesium. The relation

$$\sigma=\tfrac{1}{2}(1-\beta^2)/(1+\beta^2)$$

can then be used to determine $|\beta|$. Bohr notes that the sign of β is not determined by this equation, although knowledge of the sign is necessary to obtain ζ from (19). The positive sign is to be used for β when $I=l+1/2$, whereas l is to be negative if $I=l-1/2$. Finally, α_s is given by

$$\alpha_s=\sigma g_s/[(I+1)g].$$

[35] R. J. Blin-Stoyle, Revs. Modern Phys. 28, 75 (1956).

Using these relations, we obtain for Cs^{133}, Cs^{135}, and Cs^{137} the values: $\sigma=-0.149$, -0.107, -0.076; $\beta=-1.36$, -1.24, -1.17; $\zeta=1.92$, 2.64, 3.80; and $\alpha_s=-0.25$, -0.17, -0.12. The anomalies are again calculated from (16).

Model 4

Davidson and Feenberg[36] ascribe the departure of the magnetic moment from the Schmidt limit to a mixing of the single-particle wave function corresponding to one Schmidt limit with a many-particle wave function corresponding to the other limit. Such a wave function has an orbital angular momentum differing by 1 from the single-particle l value, but the same spin. Its corresponding g_l is taken as Z/A, i.e., the Margenau-Wigner (M-W) limit.[37] A many-particle wave function is necessary because the corresponding single-particle wave function has a parity opposite from that required for mixing with the original single-particle wave function. The proper mixture is obtained by requiring that

$$g_{\text{exp}}=ag_{\text{Schmidt}}(g_{7/2})+(1-a)g_{\text{M-W}}(f_{7/2})\qquad(22)$$

for the odd-proton cases. Here a is the fraction of single-particle admixture. The values g_{Schmidt} and $g_{\text{M-W}}$ are obtained from (17), with $g_s=g_s^{\text{free}}$ for both parts of (22), and $g_l=1$ and Z/A for the two parts. The individual α_i' are obtained as before but the total contribution is now $(\alpha_i)_{\text{Schmidt}}=a(\alpha_i')_{\text{Schmidt}}$ and $(\alpha_i)_{\text{M-W}}=(1-a)(\alpha_i')_{\text{M-W}}$. We have denoted by primes the spin and orbital contributions for states with no admixtures. For the $g_{7/2}$ proton, $\zeta=5/7$ as before. For the uniform spherically symmetrical distribution of the Margenau-Wigner limit, the angular asymmetry factor $\zeta=0$, and (from Sec. V-A) $(R^2/R_0^2)_{\text{Av}}=3/5$. From (16) and (22), therefore, we have

$$-\epsilon=[1.271(\alpha_s)_{\text{Schmidt}}+0.62(\alpha_l)_{\text{Schmidt}}]\times(0.90)(1.37)+[(\alpha_s)_{\text{M-W}}+0.62(\alpha_l)_{\text{M-W}}](0.60)(1.37).\qquad(23)$$

It is found that $g_{\text{Schmidt}}=0.490$, $g_{\text{M-W}}\approx1.020$, $a=0.537$, 0.453, 0.391 for Cs^{133}, Cs^{135}, and Cs^{137}, $(\alpha_s')_{\text{Schmidt}}=-1.270$, and $(\alpha_s')_{\text{M-W}}\approx0.785$. It is readily found that this model is not applicable to Cs^{134}.

[36] J. P. Davidson and E. Feenberg, Phys. Rev. 89, 856 (1953).
[37] H. Margenau and E. P. Wigner, Phys. Rev. 58, 103 (1940).

C. Discussion

A comparison of the theoretical values of Table V with the experimental values shows that no particular model is strongly favored. All of them, however, give order-of-magnitude agreement. This, along with the previous observations[38] that the actual values of the moments themselves do not change significantly by the addition of two neutrons to Cs^{133} and then to Cs^{135}, lends support to the single-particle model. It can be seen, however, that a change of less than 10% in the ϵ's could bring agreement between the Δ of a particular model and the experimental value. All of the models lead to a monotonic variation of the ϵ's with the magnetic moments, so that none predicts the correct sign of the Cs^{137}–Cs^{135} anomaly. This would require $\epsilon^{137} > \epsilon^{135}$, while $\epsilon^{135} < \epsilon^{133}$. It is possible that part of the discrepancy might be accounted for even with the above models if we assume a decrease in the value of $(R^2/R_0^2)_{\text{Av}}$ for Cs^{137}. This appears plausible, since Cs^{137} contains 82 neutrons, a magic number leading to a tightly bound closed neutron shell. It is doubtful, however, that the total reduction of 5% to 10% in $(R^2/R_0^2)_{\text{Av}}$ is ascribable to this effect. An admixture of $d_{5/2}$ protons with its smaller value of $(R^2/R_0^2)_{\text{Av}}$ might be more plausible. It can be shown that in this way it is possible to obtain agreement in magnitude and sign for the anomalies in the three isotopes.[39]

A mixed $d_{5/2}-g_{7/2}$ configuration for the Cs^{134} proton was suggested by Sunyar, Mihelich, and Goldhaber[40] on the basis of shell model calculations and the decay scheme of the nuclear isomeric level in Cs^{134}. We see from Table V that the experimental value $\Delta=0.169 \pm 0.030\%$ lies about halfway between the pure single-particle value $\Delta=0.205\%$ and the mixed-configuration value $\Delta=0.113\%$. Hence there is no significant disagreement introduced by the proposed Cs^{134} ground state.

From this and previous work on hfs anomalies, correct orders of magnitude and sign—with the interesting exception for Cs^{137}—are obtained, but closer agreement requires a better evaluation of $(R^2/R_0^2)_{\text{Av}}$, perhaps from higher-order nuclear moments, as well as a more formal inclusion in the theory of the effects of nuclear configuration interactions.

ACKNOWLEDGMENTS

We wish to thank Professor J. R. Zacharias for his continued support and interest in the performance of this experiment. We are also indebted to Professor B. Bederson for his contribution in the initial stages of the experiment, to Professor J. G. King for his valuable advice, and to Dr. J. Eisinger for helpful discussions. Finally, we wish to thank Professor A. Bohr, Professor B. T. Feld, Professor V. F. Weisskopf, and Dr. K. Gottfried for discussions on the theoretical part.

APPENDIX A. TRANSITIONS USED IN THE EXPERIMENT

For $\Delta F=\pm 1$ transitions, we have, from Eq. (9),

$$\nu = g_I\mu_0 H_C(m_+ - m_-) + \frac{\Delta\nu}{2}\left[\left(1+\frac{4m_+x}{2I+1}+x^2\right)^{\frac{1}{2}} + \left(1+\frac{4m_-x}{2I+1}+x^2\right)^{\frac{1}{2}}\right], \quad (24)$$

where m_+ and m_- are the values of m_F in the upper and lower F-states, respectively. For $x \ll 1$, where the experiments were performed, the nuclear term can be neglected, and an expansion of the second term to x^2 yields

$$\nu = \frac{\Delta\nu}{2}\left(2+\frac{2x}{2I+1}(m_+ + m_-) + x^2\left[1-\frac{2}{2I+1}(m_+^2+m_-^2)\right]\right). \quad (25)$$

The m_F values of the transitions used are given in Table VI. The m-dependence of the quadratic term is negligible or zero for the transitions used. In terms of the field calibrating transition,

$$\nu_z(\Delta F=0, \quad m_F=-|F_{\max}| \leftrightarrow m_F=-|F_{\max}|+1)$$

Eq. (25) yields

$$\Delta\nu = \nu - \nu_z(m_+ + m_-) - 32(\nu_z^2/\Delta\nu), \quad (26)$$

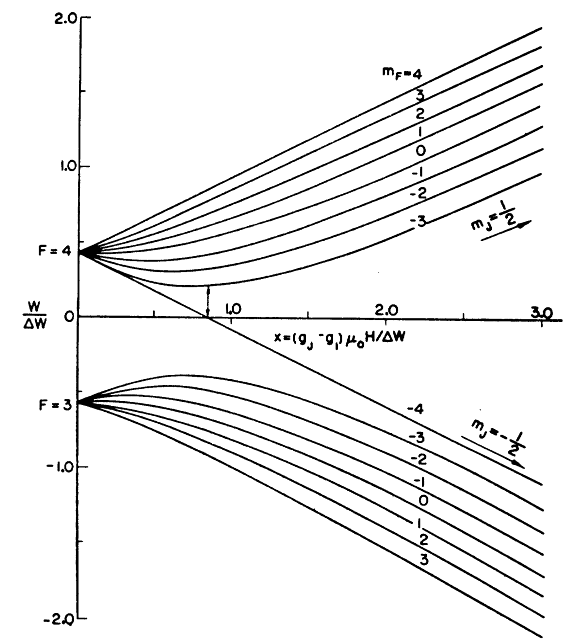

FIG. 14. Energy-level diagram for $J=1/2$, $I=7/2$, drawn for a positive magnetic moment.

[38] J. M. Blatt and V. F. Weisskopf, *Theoretical Nuclear Physics* (John Wiley and Sons, Inc., New York, 1952), p. 773.
[39] V. Jaccarino and H. H. Stroke (unpublished).
[40] Sunyar, Mihelich, and Goldhaber, Phys. Rev. **95**, 570 (1954).

TABLE VI. $\Delta F=\pm 1$ transitions used for $\Delta\nu$ measurements.

Isotope	m_+	m_-
Cs^{134}	$+1/2$	$-1/2$
	$-1/2$	$+1/2$
Cs^{135}, Cs^{137}	$+1$	0
	0	$+1$
	0	-1
	-1	0
	0	0

for $I=7/2$ and

$$\Delta\nu=\nu-\nu_z(m_+ + m_-)-(81/2)(\nu_z^2/\Delta\nu) \tag{27}$$

for $I=4$.

Direct g values are obtained by observing $\Delta F=0$ transitions between states that have $m_{1+}=m_{2-}$, and $m_{2+}=m_{1-}$, where $+$ and $-$ denote the $F=I\pm 1/2$ states and 1 and 2 the higher- and lower-energy states. From (9), we have

$$\begin{aligned}\nu_+ &= g_I\mu_0 H+\frac{\Delta\nu}{2}\left[\left(1+\frac{4m_{1+}x}{2I+1}+x^2\right)^{\frac{1}{2}} -\left(1+\frac{4m_{2+}x}{2I+1}+x^2\right)^{\frac{1}{2}}\right],\\ \nu_- &= -g_I\mu_0 H-\frac{\Delta\nu}{2}\left[\left(1+\frac{4m_{2+}x}{2I+1}+x^2\right)^{\frac{1}{2}} -\left(1+\frac{4m_{1+}x}{2I+1}+x^2\right)^{\frac{1}{2}}\right].\end{aligned} \tag{28}$$

TABLE VII. $\Delta F=0$ transitions used in g measurements.

Isotope	m_{2-}, m_{1+}	m_{1-}, m_{2+}
Cs^{133}	-1	-2
Cs^{134}	$-3/2$	$-5/2$
Cs^{135}	-1	-2
Cs^{137}	-1	-2

The difference between these two transitions is

$$\nu_+ - \nu_- = 2g_I\mu_0 H. \tag{29}$$

The value of g_I can then be obtained when H is known. The transitions used are listed in Table VII. The spin 7/2 energy level diagram is shown in Fig. 14.

APPENDIX B. EXPERIMENTAL DATA

The results of the individual runs are given in Tables VIII to XIII.

TABLE VIII. Measurements of $\Delta\nu$.

Isotope	Transition	ν_+ Mc/sec	ν_- Mc/sec	ν_z Mc/sec	$\Delta\nu$ Mc/sec	Notes
135	± 1 Zeeman	9725.916	9722.150	1.890	9742.021	
	± 1 Zeeman	9725.914	9722.147	1.893	9724.019	a, b
	± 1 Zeeman	9725.526	9722.532	1.494	9724.022	
	± 1 Zeeman	9725.502	9722.518	1.460	9724.003	c
	± 1 Zeeman	9727.314	9720.806	3.260	9724.026	
	$0\leftrightarrow 0$	9724.087	9724.017	2.792	9724.026	
137	± 1 Zeeman	10 118.632	10 112.493	3.071	10 115.534	b
	± 1 Zeeman	10 118.798	10 112.308	3.240	10 115.521	b
	$0\leftrightarrow 0$	10 115.578	10 115.519	2.712	10 115.526	
134	-5 Zeeman		10 458.317	3.026	10 473.412	d
	-1 Zeeman		10 470.562	3.026	10 473.553	
	$\pm\frac{1}{2}\leftrightarrow\mp\frac{1}{2}$		10 473.659	2.829	10 473.628	a
	$\pm\frac{1}{2}\leftrightarrow\mp\frac{1}{2}$		10 473.655	2.829	10 473.624	

[a] Full resonance curve obtained.
[b] Calculation using Eq. (24)—otherwise (26) and (27) are used.
[c] The value of H_c could not be well determined in this run.
[d] This first measurement was not made with optimum rf power and the field was determined from the average of ν_z in two adjacent rf loops.

TABLE IX. g^{135}/g^{133}—line method.

Time (min)	Cs^{133} ν_+(Mc/sec)	Cs^{133} ν_-(Mc/sec)	Cs^{133} $2g_I\mu_0 H$(Mc/sec)	Cs^{135} ν_+(Mc/sec)	Cs^{135} ν_-(Mc/sec)	Cs^{135} $2g_I\mu_0 H$(Mc/sec)
0		1236.5047				
35	1246.2647	1236.5077[a]	9.7570			
45		1236.5085				
70					1307.8632	
78				1318.1850[a]	1307.8632[a]	10.3218
85				1318.1843		
95		1236.5123				
110	1246.2642	1236.5134[a]	9.7508			
142	1246.2632					
149	1246 2630[a]	1236.5157	9.7473			
175				1318.1747		
190				1318.1731[a]	1307.8625	10.3106
					$g^{135}/g^{133}=1.05820\pm 0.00010$	

[a] Linear time extrapolation.

TABLE X. g^{135}/g^{133}—doublet method.

Run	Total time min	$2g_I\mu_0 H$ Cs^{135} Mc/sec	No. of meas.	Standard deviation kc/sec	$2g_I\mu_0 H$ Cs^{133} Mc/sec	No. of meas.	Standard deviation kc/sec	g^{135}/g^{133}	Standard deviation	Remarks
1	100	10.4892	6	2.5	9.9114	8	1.1	1.05830	0.00027	Runs 1–3 low
2	60	10.4776	8	1.9	9.9010	8	1.1	1.05824	0.00022	abundance
3	180	10.6704	8	2.3	10.0824	11	1.2	1.05832	0.00026	samples
4	190	10.6997	32	1.1	10.1113	25	0.8	1.05820	0.00013	
5	140	10.7204	28	1.1	10.1318	22	1.2	1.05810	0.00017	
					Weighted average of all 6 runs			1.05820	0.00008	

TABLE XI. g^{137}/g^{133} data.

Run	Total time min	$2g_I\mu_0H$ Cs^{137} Mc/sec	No. of meas.	Standard deviation kc/sec	$2g_I\mu_0H$ Cs^{133} Mc/sec	No. of meas.	Standard deviation kc/sec	g^{137}/g^{133}	Standard deviation	Remarks
1	320	10.9758	16	1.5	9.9741	14	1.3	1.10043	0.00019	Optimum
2	120	11.2558	18	2.7	10.2305	8	1.1	1.10022	0.00029	field run
3	125	10.7774	14	2.7	9.7940	8	1.9	1.10041	0.00033	
					Weighted average			1.10037	0.00015	

TABLE XII. g^{137}/g^{135} data.

Run	Total time min	$2g_I\mu_0H$ Cs^{137} Mc/sec	No. of meas.	Standard deviation kc/sec	$2g_I\mu_0H$ Cs^{135} Mc/sec	No. of meas.	Standard deviation kc/sec	g^{137}/g^{135}	Standard deviation	Remarks
1	160	10.8505	29	1	10.4334	19	0.9	1.03998	0.00014	Nonlinear
2	95	10.7864	12	0.8	10.3690	12	0.8	1.04008	0.00011	field drift
3	250	10.7487	54	1	10.3345	43	0.9	1.04008	0.00013	runs 1, 2
					Weighted average			1.04005	0.00008	

TABLE XIII. g^{134}/g^{133} data.

Run	Total time min	$2g_I\mu_0H$ Cs^{134} Mc/sec	No. of meas.	Standard deviation kc/sec	$2g_I\mu_0H$ Cs^{133} Mc/sec	No. of meas.	Standard deviation kc/sec	g^{134}/g^{133}	Standard deviation	Remarks
1	230	9.6482	12	2.6	9.5106	16	1.2	1.01447	0.00029	Lower in-
2	126	9.4173	5	3.9	9.2856	9	1.4	1.01418[a]		tensity runs
3	80	9.5720	3	1.6	9.4360	8	0.8	1.01441[a]		2, 3
					Weighted average			1.01447	0.00029	

[a] Too few measurements to calculate a standard deviation. These results are given only for completeness.